

Compact Microstrip Dual-Band Bandpass Filters Design Using Genetic-Algorithm Techniques

Ming-Iu Lai, *Student Member, IEEE*, and Shyh-Kang Jeng, *Senior Member, IEEE*

Abstract—An optimization scheme based on hybrid-coded genetic-algorithm (GA) techniques is presented to design compact dual-band bandpass filters with microstrip lines. A representation scheme is proposed to represent an arbitrary microstrip circuit as a set of data structures. Each data structure in the set describes a simple two-port network with the corresponding connection method and electrical parameters. The optimization algorithm based on conventional GAs is then applied to simultaneously search for the appropriate circuit topology and the corresponding electrical parameters with dual-band characteristic. Two examples are designed and implemented to validate the proposed algorithm. In the first example, the 3-dB fractional bandwidth of the low and high bands is 35% and 17%, respectively. It has return losses larger than 10 dB from 2.14 to 2.96 and 5.14 to 6.06 GHz. In the second example, the 3-dB fractional bandwidth of the low and high bands is 9.9% and 7.9%, respectively. The return losses are larger than 10 dB from 3.37 to 3.64 and 5.27 to 5.62 GHz. The sizes of the proposed filters are nearly half as small as those of the filters presented before. All the studies are completed on a computer with a 2.4-GHz microprocessor, and the computing time of two examples is 6 and 3 min, respectively.

Index Terms—Bandpass filters, circuit topology, genetic algorithm (GA), microstrip circuit.

I. INTRODUCTION

WIRELESS products such as wireless local area networks (WLANs), Bluetooth, etc. gradually become standard facilities in notebooks. In order to pursue more convenient and compact products, the demands for multifunctional RF transceiver systems increase dramatically. In this trend, the development of multifunctional components like antennas and filters plays an important role. In theory, a dual-band bandpass filter can be realized by cascading a bandpass and bandstop filter [1]. Nevertheless, this design approach is confronted by two difficulties. First, the bandpass filter needs to be with very wide passband if the ratio of the high-band central frequency to the low-band central frequency is high. Second, since the bandpass and bandstop filters are designed separately and then cascaded to fulfill the dual-band characteristics, the resultant circuit topology is large in size and, therefore, fails in compact

design. Wada *et al.* [2], [3] studied the behavior of open-ended resonators and their application to microwave filters. They successfully applied the open-ended resonators and some lumped capacitors to design a bandpass filter with two narrow passbands [4]. However, their filter was simulated using ideal lumped capacitors and there was no measured result. When realizing the filter, the use of chip capacitors may degrade the circuit's performance and cause some unwanted effects. Accordingly, new methods to design compact and high-performance dual-band bandpass filters are highly desirable.

Various optimization techniques such as the gradient-based method [5], space mapping [6], [7], and neural networks [8] are available to design microwave circuits. Hsu and Huang [9] proposed a simulated annealing algorithm to design dual-wide-band microstrip line filters for WLAN applications. This approach worked on the electrical parameters based on a given circuit topology. A great deal of effort has been made on searching for the design parameters based on a given circuit topology. Only a few attempts thus far have been made at developing an algorithm capable of searching for the circuit topology, as well as the electrical parameters simultaneously.

Genetic algorithms (GAs), first introduced by Holland in 1975, have been widely used in science and engineering problems [10], [11]. It also proves to be useful for solving complex electromagnetic problems [12]–[18]. For microwave filters synthesis, Peik and Chow [16] focused on searching for the optimal electrical parameters based on a given circuit topology. Nishino and Itoh [17], [18] proposed a scheme to describe the physical parameters and topology of the circuit composed of microstrip-line segments and then integrated this representation scheme with conventional GAs. Many filters with several passbands and stopbands were presented. Nevertheless, since the representation scheme merely modeled the transmission-line segments with equal width and open-circuited shunt stubs, it is difficult to realize dual-band bandpass filters with sharp cutoff in the passbands, as well as good rejections in the stopbands. The goal of this paper is to then explore an efficient computer-aid tool, which does not require human intervention, to synthesize dual-band bandpass filters including the circuit topology, as well as the corresponding electrical parameters.

As a beginning, a scheme is proposed to represent an arbitrary microstrip circuit as a set of data structures. Each data structure in the set describes a simple two-port network with the corresponding connection method and electrical parameters. The optimization algorithm based on conventional GA is then applied to simultaneously search for the appropriate circuit topology and the corresponding electrical parameters with a dual-band characteristic. The details of the algorithm are addressed in Sec-

Manuscript received December 8, 2004; revised June 22, 2005. This work was supported by the National Science Council, Taiwan, R.O.C., under Grant NSC 93-2213-E-002-091 and by the Department of Industrial Technology, Ministry of Economic Affairs, Taiwan, R.O.C., under Technology Development Program of Academic 93-EC-17-A-05-S1-020.

M.-I. Lai is with the Graduate Institute of Communication Engineering, National Taiwan University, Taipei, 10617 Taiwan, R.O.C. (e-mail: milai1102@yahoo.com.tw).

S.-K. Jeng is with the Graduate Institute of Communication Engineering and the Department of Electrical Engineering, National Taiwan University, Taipei, 10617 Taiwan, R.O.C. (e-mail: skjeng@ew.ee.ntu.edu.tw).

Digital Object Identifier 10.1109/TMTT.2005.860327

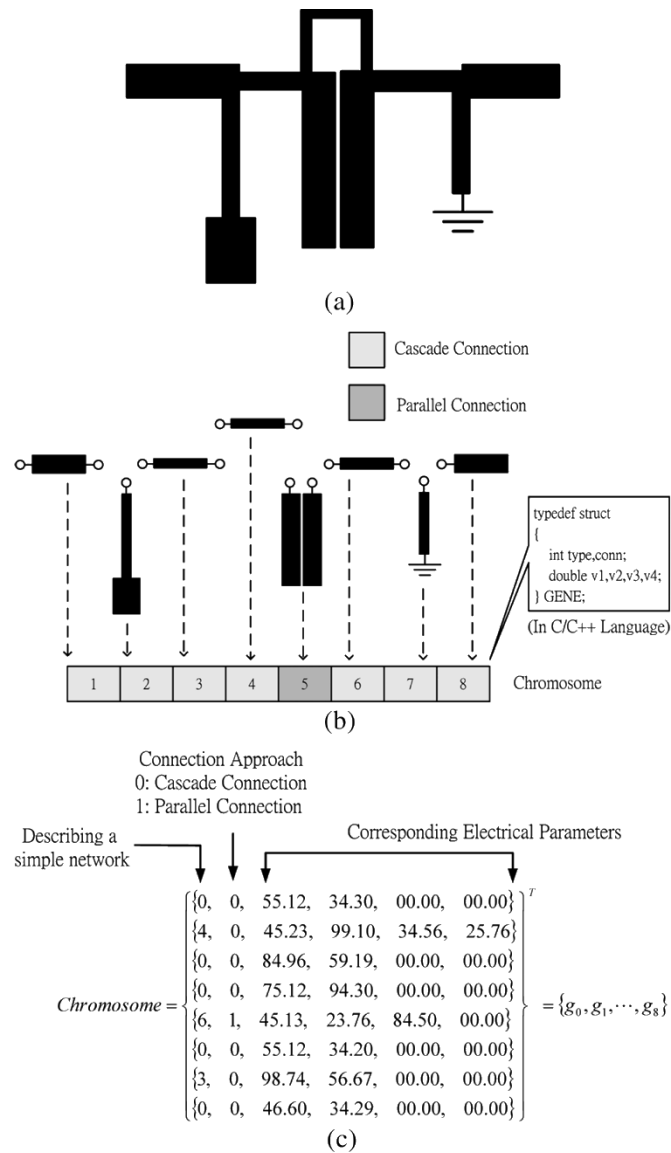


Fig. 1. Representation scheme in the proposed algorithm. (a) A typical passive microstrip circuit. (b) Decomposition of the circuit in (a) into basic circuit elements. (c) Chromosome of the circuit in (a), a set of structures.

tion II. Section III demonstrates two compact dual-band bandpass filters to validate the algorithm. Finally, some conclusions are given in Section IV.

II. THEORY

A. Representation Scheme

As illustrated in Fig. 1, an arbitrary two-port microstrip circuit [1], [19]–[22] can be decomposed into basic circuit elements. The data structure shown in Fig. 1(b) is then applied to describe such a basic circuit element. It is composed of three parts. The first part is coded in an integer representing the topology of a basic element. The second part is coded in an integer representing the way of connection to the previous element. The third part consists of many real numbers describing the corresponding electrical parameters of the element. Table I lists the details of the basic circuit elements. In the algorithm,

TABLE I
DETAILS OF THE BASIC ELEMENTS IN THE PROPOSED ALGORITHM

| Category | Type | Name | Network Topology | Possible Connections | Electrical Parameters |
|------------------------|------|-----------|------------------|----------------------|-----------------------------------|
| Basic Circuit Elements | 0 | TL | | Cascade and Parallel | $Z_{o1} \theta_1$ |
| | 1 | CTL | | Cascade | $Z_{oo} \Delta Z \theta_1$ |
| | 2 | Sh_TL_OC | | Cascade | $Z_{o1} \theta_1$ |
| | 3 | Sh_TL_SC | | Cascade | $Z_{o1} \theta_1$ |
| | 4 | Sh_TL2_OC | | Cascade | $Z_{o1} \theta_1 Z_{o2} \theta_2$ |
| | 5 | Sh_TL2_SC | | Cascade | $Z_{o1} \theta_1 Z_{o2} \theta_2$ |
| Special Element | 100 | Empty | | Cascade | None |

Z_{oi} : characteristic impedance of the i th transmission line section.
 θ_i : electrical length concerned at f_0 of the i th transmission line section in degrees.
 Z_{oo} : odd-mode characteristic impedance. Z_{oe} : even-mode characteristic impedance. ΔZ : $Z_{oe} - Z_{oo}$.

we define a structure as a *gene* and a set of structures as a *chromosome*. A special gene called *Empty* is introduced, which enables the representation scheme to be capable of describing a circuit with an arbitrary number of basic circuit elements and orders. With this approach, an arbitrary two-port network can be represented by a set of structures. The design problem can be formulated as

$$\mathbf{g}^* = \arg \left(\min_{\mathbf{g}} U(\mathbf{S}(\mathbf{g})) \right) \quad (1)$$

where \mathbf{g} denotes a chromosome, as illustrated in Fig. 1(c), and $\mathbf{S}(\mathbf{g})$ is the scattering matrix obtained by electromagnetic simulation. U is the objective function to be minimized and \mathbf{g}^* is the appropriate chromosome.

B. Design Constraints

During synthesis in order to avoid unreasonable electrical parameters in a chromosome, it is necessary to assign upper and lower limits according to various designs. The flowchart of the constraint testing is shown in Fig. 2. The first step is to check the values of electrical parameters in a chromosome. Since a randomly generated chromosome may represent an unreasonable network, additional attention should be paid in advance to identify whether the circuit topology is a reasonable network and to remove the troublesome chromosome from a solution pool. For example, if the way of connection of a circuit element is parallel, but the circuit topology of the previous element is a shunt element, it is trivial to calculate the frequency responses for such a circuit topology. The junction problem is another issue when realizing a chromosome to a real microstrip circuit. Common junctions in microstrip circuits are step-, tee-, and cross-junctions, and others may result in problems in circuit implementation. The algorithm for checking the circuit topology represented by a chromosome is shown in Appendix A. For the chromosomes representing a reasonable network, user-defined constraints such as the area of a circuit and the number of stubs are

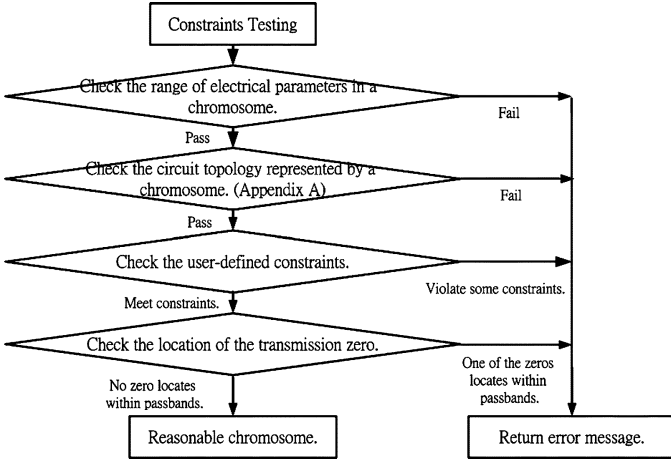


Fig. 2. Flowchart for constraint testing.

then checked. These constraints are defined according to individual design requirements.

The following step is to check the location of the transmission zero, which falls within the bandstop regions. From this step, we can easily predict the electrical performance of a randomly generated chromosome. This procedure not only sieves out the inferior chromosome from a solution pool, but also saves the computing time for evaluating the frequency responses of a circuit. For a chromosome with an open- or short-circuited shunt stub, the location of the transmission zero can easily be determined by

$$f_n = \frac{(2n-1)\pi}{2\theta} f_0 \quad (\text{for type Sh_TL_OC}) \quad (2)$$

$$f_n = (n-1)\frac{\pi}{\theta} f_0 \quad (\text{for type Sh_TL_SC}) \quad (3)$$

$$f_n \cong \frac{(2n-1)\pi}{2(\theta_1 + \theta_2)} f_0 \quad (\text{for type Sh_TL2_OC}) \quad (4)$$

$$f_n \cong (n-1)\frac{\pi}{\theta_1 + \theta_2} f_0 \quad (\text{for type Sh_TL2_SC}) \quad (5)$$

where θ , θ_1 , and θ_2 are the electrical length of the stubs in radians, f_0 denotes the reference frequency, and $n = 1, 2, \dots$

C. Definition of Fitness Value

The transmission-line models are used to calculate scattering parameters in order to effectively evaluate the frequency response of a chromosome. The algorithm for evaluating the scattering parameters of a chromosome is shown in Appendix B. The fitness value is defined by

$$F = \sum_{i=1}^N w_i f_i \quad (6)$$

where w_i represents the weighting value at the i th sampling point, f_i is the square of the difference between the magnitude of the calculated scattering parameter and the desired value at the i th sampling point, and N is the number of sampling points.

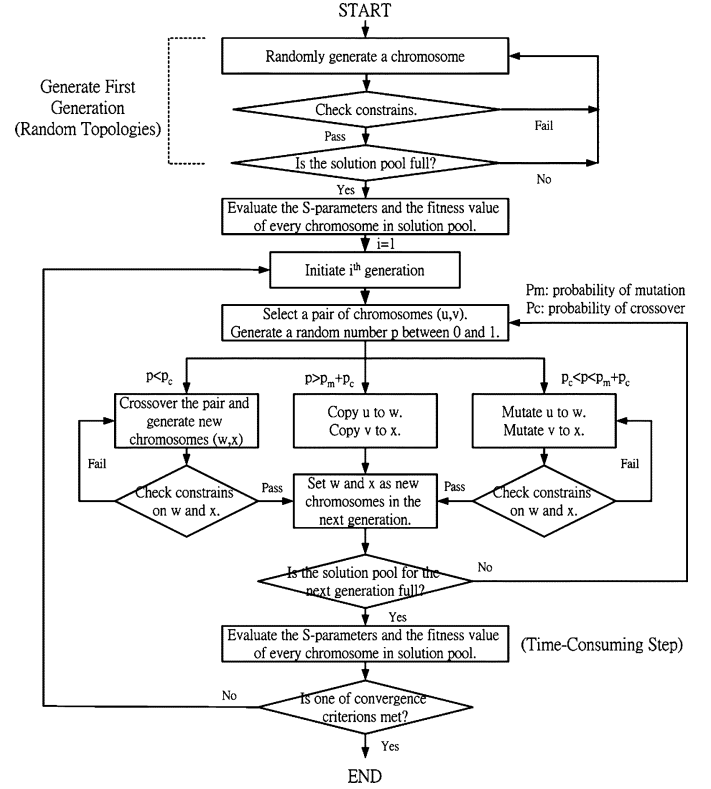


Fig. 3. Flowchart of the proposed algorithm.

In a multiobject case, the overall fitness value can be expressed by [11]

$$S = \left[\sum_{i=1}^M (W_i F_i)^2 \right]^{\frac{1}{2}} \quad (7)$$

where W_i is the weighting value on the i th fitness value, M is the number of fitness values, and F_i is the i th fitness value. After evaluating the fitness of every chromosome within a solution pool, we apply the fitness-sharing algorithm [11] based on genotypic similarity to adjust the value in order to keep the diversity of chromosomes. The linear fitness-scaling algorithm [10] is then used to automatically shift the fitness values to make them work well for a given selection method.

D. GA

Selection, crossover, and mutation are the basic operators in GAs. Fig. 3 is the flowchart of the proposed algorithm. The first step is to generate n random chromosomes satisfying all constraints discussed in the above paragraph. Following the scattering parameters and fitness value of every chromosome within the solution pool are evaluated. For the selection operator, the proportionate selection scheme is adopted [10], and the probability of selecting the i th chromosome is defined as

$$p_i = \frac{S'_i - S'_j}{\sum_j (S'_i - S'_j)} \quad (8)$$

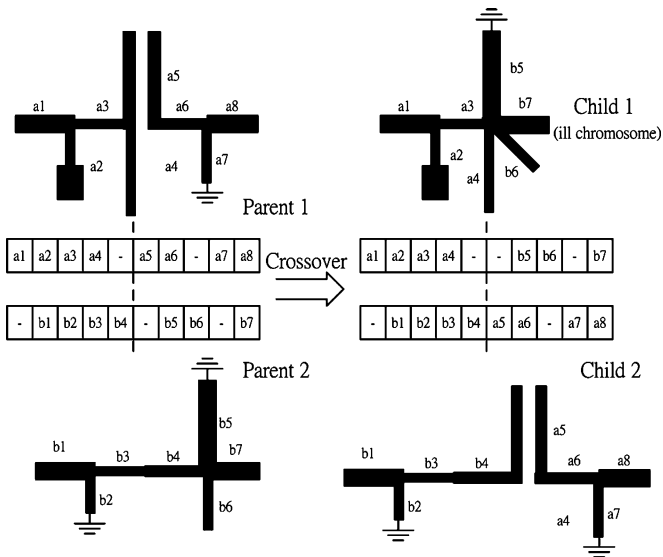


Fig. 4. Illustration of the one-point crossover operator in the proposed algorithm.

where S'_i and S'_{\max} denote the fitness value of the i th chromosome and the maximal fitness value, respectively. Note that the fitness values have been shifted using the sharing and scaling algorithms. Once a pair of chromosomes is selected, the crossover and mutation genetic operators are used to create new chromosomes for the next generation. In this study, the probability to perform the crossover and mutation operators is specified as 0.6 and 0.1, respectively [23]. For other possibilities, the selected pair directly copies to the next generation.

The proposed algorithm applies the one-point crossover method [10], as illustrated in Fig. 4. Unfortunately, such an operator may generate ill offspring. To avoid this, the constraint testing in Fig. 2 is performed on the offspring. Step- and topology-mutation operators are both applied to produce offspring. The step-mutation operator [19] keeps the circuit topology and merely changes the electrical parameters in a chromosome, as shown in Fig. 5. The new electrical parameter in a chromosome is defined as

$$x'_i = [1 + aN]x_i \quad (9)$$

where x_i is the original electrical parameter and N is a random variable in uniform distribution with a value from -1 to 1 . The variable a is interpreted as a mutation step size whose initial value is specified as 0.3. The step size of the next generation is adaptive according to the successful rate of the step mutations in this generation. To introduce more circuit topologies into a solution pool, we create the topology-mutation operator, which randomly selects one gene in a chromosome to change the circuit topology, as well as the corresponding parameters, as shown in Fig. 6. Similar to the crossover operator, the offspring should meet the constraints. The probability to execute two mutation operators is equal in the beginning of the algorithm. However, the topology-mutation operator is disabled when the successful rate of this operator is less than 5% in five recent generations.

When the evolution count reaches the maximum value or one of the fitness value of a chromosome in a solution pool gets in the target fitness value, the algorithm terminates. Here, we

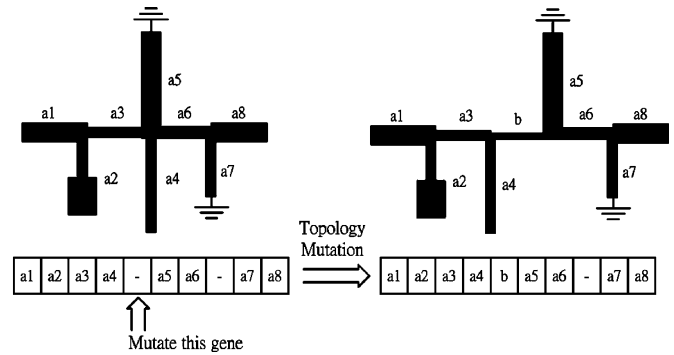


Fig. 5. Illustration of the step mutation operator.

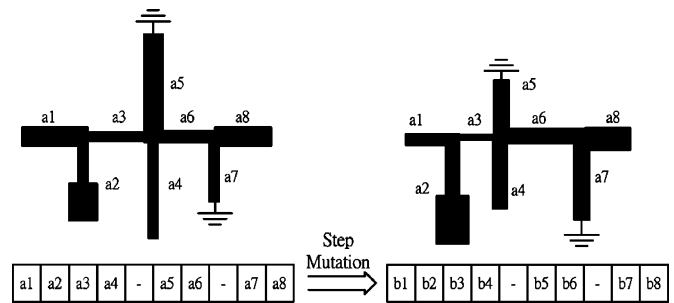


Fig. 6. Illustration of the topology mutation operator.

specify the target fitness value as zero. In the generation evolution process, evaluating the scattering parameters is the most time-consuming step.

III. DESIGN EXAMPLES

Here, two dual-band bandpass filters are designed and implemented to validate the proposed algorithm. The first filter is for IEEE 802.11 a/b/g WLAN systems and the designed specifications are taken as

Return losses within 2.1–2.9 and 5.1–5.9 GHz > 10 dB
Rejections within dc: 1.5, 3.5–4.5, and 6.5–8.0 GHz > 40 dB.

This filter possesses a sharp cutoff in the passbands and very good rejection in the stopbands. It covers all industrial–scientific–medical (ISM) and Unlicensed National Information Infrastructure (U-NII) bands. The specifications of the second filter are given as

Return losses within 3.4–3.6 and 5.4–5.6 GHz > 10 dB
Rejections within 2.0–3.0, 4.0–5.0, and 6.0–7.0 GHz > 20 dB.

Differing from [17], whose rejections are merely required to be larger than 15 dB within 2.4–2.6 and 4.4–4.6 GHz, the above specifications aim at obtaining a dual-band bandpass filter with a sharper cutoff in the passbands and better rejection in the stopbands.

The desired scattering parameters of the design examples according to the forgoing specifications are described by piecewise-linear functions in Fig. 7, where the weighting value of each linear region is also depicted. For a sampling point within the shading portions in this figure, the score of the point is set to zero if the evaluated value is smaller than the desired value.

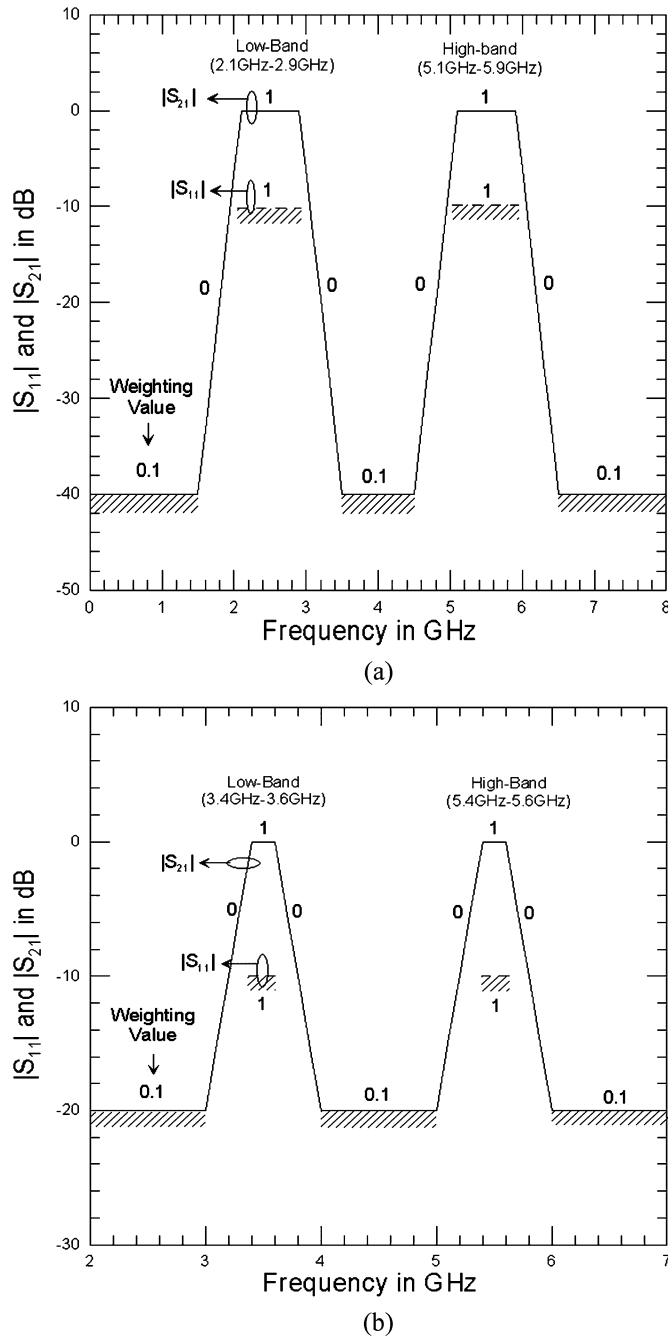


Fig. 7. Desired frequency responses of the examples. (a) Example 1. (b) Example 2.

The weighting values are carefully specified to obtain better frequency responses.

Two filters were fabricated on an RO4003 substrate with thickness $h = 0.508$ mm and relative dielectric constant $\epsilon_r = 3.38$. Due to the tolerance of the fabrication, the minimum width is limited to 0.2 mm, which corresponds to a microstrip line with a characteristic impedance of 110 Ω . Meanwhile, to lower the junction discontinuity effects, the maximum line width is chosen to be 2 mm, which corresponds to a microstrip line with a characteristic impedance of 40 Ω . To avoid coupling between adjacent stubs, the minimum electrical lengths of the TL and CTL are chosen to be 30° . Table II summarizes the upper and lower limits of the electrical parameters

TABLE II
UPPER AND LOWER LIMITS OF THE ELECTRICAL
PARAMETERS IN THE DESIGN EXAMPLES

| Type Name | Z (Ohms) | Z_{o0} (Ohms) | ΔZ (Ohms) | Theta(@4GHz) |
|-------------------------|----------|-----------------|-------------------|--------------|
| TL | 40-110 | - | - | 30-100 |
| Sh_TL_OC and Sh_TL_SC | 40-110 | - | - | 20-160 |
| Sh_TL2_OC and Sh_TL2_SC | 40-110 | - | - | 20-120 |
| CTL | - | 30-50 | 10-40 | 30-100 |
| CLT_OO | - | 30-50 | 10-40 | 20-160 |

TABLE III
PARAMETER SETTINGS IN THE TWO EXAMPLES

| Parameter | Design Example 1 | Design Example 2 |
|------------------------------------|---|---|
| Size of the solution pool | 200 | 200 |
| Number of the genes per chromosome | 20 | 15 |
| Maximum generations | 300 | 300 |
| Probability of crossover | 0.6 | 0.6 |
| Probability of mutation | 0.1 | 0.1 |
| Reference frequency | 4.0 GHz | 4.0 GHz |
| Calculated Frequency Range | 0.1-8.0 GHz | 1.1-7.0GHz |
| Points of Sampling | 80 | 60 |
| User Defined Constrains | $L_{total} < 500^\circ$ and $W_{total} < 350^\circ$ | $L_{total} < 200^\circ$ and $W_{total} < 300^\circ$ |
| Target Fitness Value | 0 | 0 |

Define: L_{total} and W_{total} are the overall length and width of the circuit, respectively.

TABLE IV
ELECTRICAL AND PHYSICAL PARAMETERS OF THE FIRST EXAMPLE

| No. | Name | Electrical Parameters (at $f_0 = 4$ GHz) | | | | Physical Parameters in mm (before tuning) | | | |
|-----|-----------|--|------------|----------|------------|---|-------|-------|-------|
| | | Z_o | θ_1 | Z_{o2} | θ_2 | W_1 | L_1 | W_2 | L_2 |
| 1 | Sh_TL_SC | 93.3 | 46.8 | - | - | 0.34 | 6.2 | - | - |
| 2 | Sh_TL_SC | 103.3 | 82.3 | - | - | 0.26 | 11.0 | - | - |
| 3 | Empty | - | - | - | - | - | - | - | - |
| 4 | TL | 54.4 | 96.8 | - | - | 1.0 | 12.4 | - | - |
| 5 | Empty | - | - | - | - | - | - | - | - |
| 6 | TL | 72.2 | 99.0 | - | - | 0.60 | 12.9 | - | - |
| 7 | Sh_TL2_SC | 94.4 | 63.0 | 85.6 | 36.0 | 0.33 | 8.4 | 0.42 | 4.8 |
| 8 | TL | 76.7 | 49 | - | - | 0.53 | 6.4 | - | - |
| 9 | Sh_TL2_SC | 42.2 | 51.8 | 62.2 | 23.3 | 1.51 | 6.5 | 0.80 | 3.0 |
| 10 | Sh_TL2_SC | 55.6 | 101.1 | 101.1 | 101.1 | 0.98 | 13.0 | 0.28 | 13.5 |
| 11 | TL | 106.7 | 77.9 | - | - | 0.24 | 10.5 | - | - |
| 12 | Sh_TL2_SC | 51.1 | 107.4 | 54.4 | 82 | 1.12 | 13.7 | 1.01 | 10.5 |
| 13 | TL | 100 | 72.3 | - | - | 0.29 | 9.7 | - | - |
| 14 | Sh_TL_SC | 41.1 | 95.7 | - | - | 1.57 | 12.0 | - | - |
| 15 | Sh_TL2_SC | 40 | 85.2 | 80 | 102.6 | 1.63 | 10.7 | 0.48 | 13.5 |
| 16 | TL | 71.1 | 37.9 | - | - | 0.62 | 4.9 | - | - |
| 17 | Empty | - | - | - | - | - | - | - | - |
| 18 | Sh_TL_SC | 83.3 | 106.8 | - | - | 0.45 | 14.1 | - | - |
| 19 | Empty | - | - | - | - | - | - | - | - |
| 20 | Sh_TL2_SC | 85.6 | 91.5 | 104.4 | 70.9 | 0.42 | 12.1 | 0.25 | 9.5 |

used in the two examples. The parameter settings for the two examples are then listed in Table III. Note that the constraints of the overall width of the circuit W_{total} are loose since the shunt stubs can be bent to achieve compact design.

In the first example, the best chromosome after 300 generations consists of four *Empty* elements, six thru transmission lines, and ten stubs. The achieved electrical parameters are then converted to a physical circuit. Table IV lists the electrical and physical parameters. The scattering parameters of the filter including the junction discontinuities are simulated again by the commercial circuit simulator ADS. To count the discontinuity effects and fringing capacitances, several physical parameters are slightly adjusted with the help of the commercial software. The layout, photography, and scattering parameters are shown

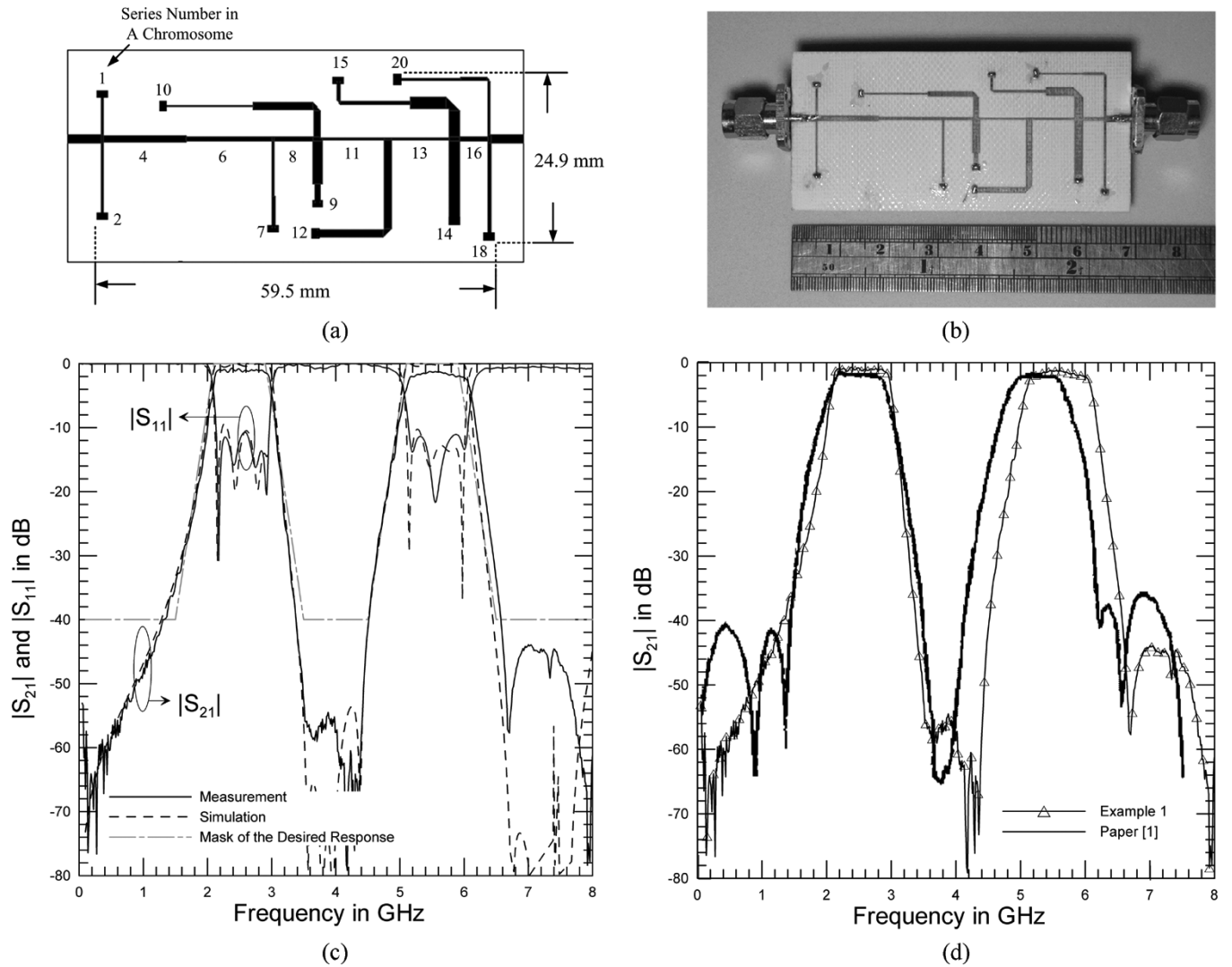


Fig. 8. First example. (a) Layout. (b) Photography. (c) Comparison between the simulated and measured scattering parameters. (d) Comparison of the measured $|S_{21}|$ of the first example with that of the filter in [1].

in Fig. 8. As seen in Fig. 8(a), the small patches at the end of the stubs are for a grounding via and the long stubs are bent to reduce the overall width of the circuit. Referring to Fig. 8(c), the return losses are larger than 10 dB and the insertion losses are smaller than 2.6 dB from 2.14 to 2.96 and 5.14 to 6.06 GHz. In addition, the rejections are greater than 40 dB from dc to 1.31, 3.38 to 4.52, and 6.58 to 8.0 GHz. The 3-dB fractional bandwidth of the low- and high-band is 35% and 17%, respectively. In Fig. 8(d), the out-of-band rejection characteristics of the proposed filter are better than those of the filter in [1] because, in our design, the desired response in the out-of-band is required to be larger than 40 dB.

In the second example, after 300 generations, there are five *Empty* elements, three thru transmission lines, and seven stubs in the best chromosome. Table V lists the electrical and physical parameters of the filter. Fig. 9(a) and (b) then shows the layout and photograph. Referring to Fig. 9(c), the return losses are larger than 10 dB and the insertion losses are smaller than 2.5 dB from 3.37 to 3.64 and 5.27 to 5.62 GHz. The rejections are greater than 20 dB from 2.03 to 3.20, 4.04 to 5.0, and 6.13 to 7.0 GHz. The 3-dB fractional bandwidth of the low- and

TABLE V
ELECTRICAL AND PHYSICAL PARAMETERS OF THE SECOND EXAMPLE

| No. | Name | Electrical Parameters (at $f_0 = 4\text{GHz}$) | | | | Physical Parameters in mm (before tuning) | | | |
|-----|-----------|---|------------|----------|------------|---|-------|-------|-------|
| | | Z_{o1} | θ_1 | Z_{o2} | θ_2 | W_1 | L_1 | W_2 | L_2 |
| 1 | Sh_TL_OC | 96.1 | 80.3 | - | - | 0.32 | 10.7 | - | - |
| 2 | Empty | - | - | - | - | - | - | - | - |
| 3 | Sh_TL2_OC | 50.9 | 52.9 | 109.6 | 97.7 | 1.13 | 6.75 | 0.22 | 13.1 |
| 4 | Empty | - | - | - | - | - | - | - | - |
| 5 | TL | 71.3 | 82.9 | - | - | 0.62 | 10.8 | - | - |
| 6 | Sh_TL2_OC | 43.3 | 119.5 | 40.3 | 46.3 | 1.45 | 15.1 | 1.62 | 5.8 |
| 7 | Sh_TL_OC | 101.6 | 77.8 | - | - | 0.27 | 10.4 | - | - |
| 8 | TL | 84.7 | 39.0 | - | - | 0.43 | 5.2 | - | - |
| 9 | Sh_TL_SC | 105.7 | 65.2 | - | - | 0.25 | 8.8 | - | - |
| 10 | TL | 40.0 | 30.4 | - | - | 1.63 | 3.8 | - | - |
| 11 | Empty | - | - | - | - | - | - | - | - |
| 12 | Sh_TL_OC | 61.0 | 160.1 | - | - | 0.83 | 20.7 | - | - |
| 13 | Sh_TL2_SC | 91.6 | 58.4 | 92.0 | 90.1 | 0.36 | 7.8 | 0.35 | 12.0 |
| 14 | Empty | - | - | - | - | - | - | - | - |
| 15 | Empty | - | - | - | - | - | - | - | - |

high-band is 9.9% and 7.9%, respectively. As seen in Fig. 9(d), it shows that the cutoff in the passbands and rejection in the stopbands are better than that of the filter in [17]. Table VI compares

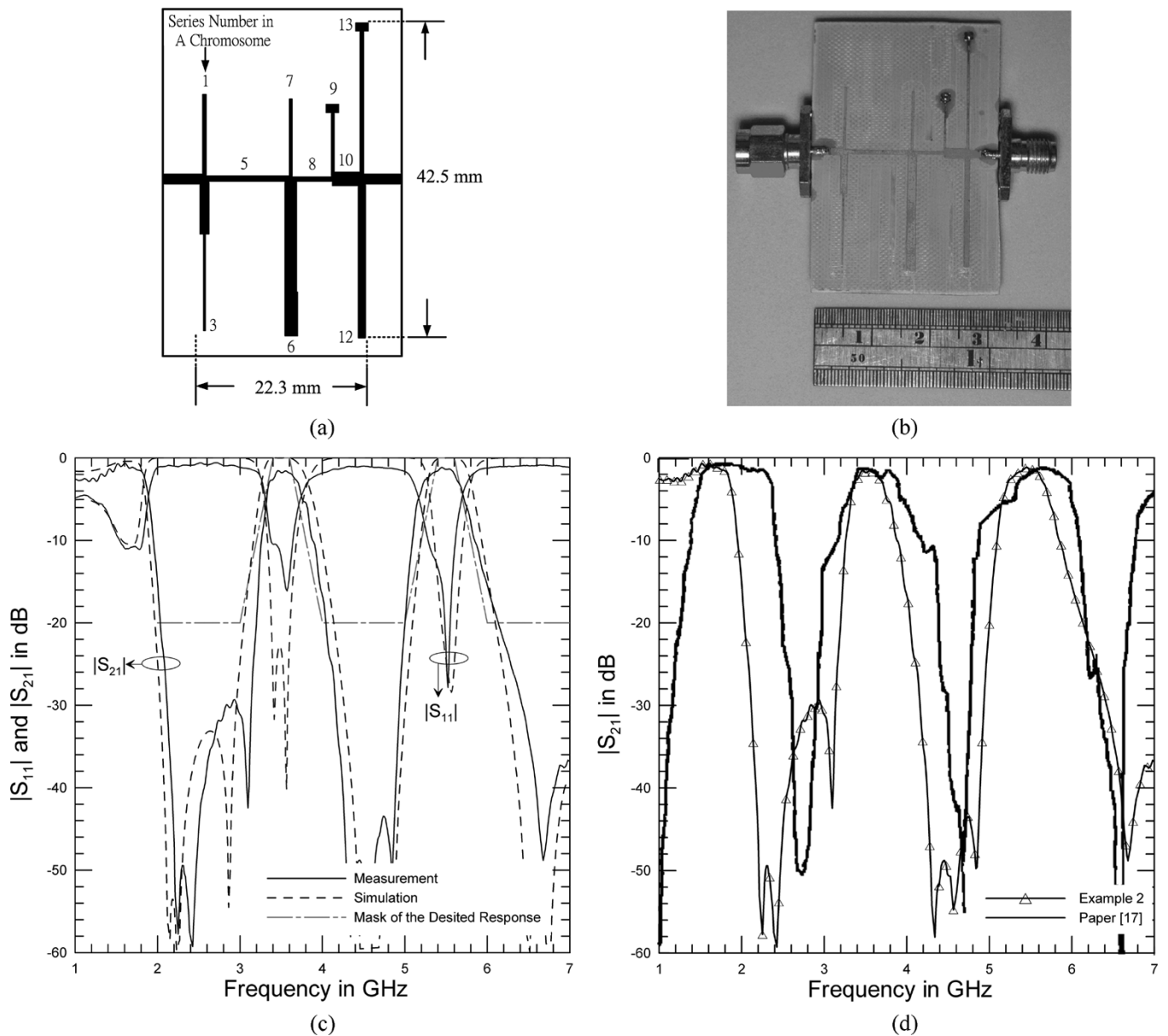


Fig. 9. Second example. (a) Layout. (b) Photography. (c) Comparison between the simulated and measured scattering parameters. (d) Comparison of the measured $|S_{21}|$ of the second example with that of the filter in [17].

TABLE VI
COMPARISON OF THE SIZES IN THIS STUDY WITH THOSE
OF THE FILTERS IN [1] AND [17]

| Filters | Substrate | | Size of Circuit | | | |
|------------|--------------|-------|-----------------|-------------|------------------------|------------|
| | ϵ_r | h(mm) | L(mm) | W(mm) | Area(mm ²) | Reduction |
| Paper [1] | 6.15 | 0.635 | 124.5 | 20.0 | 2490 | - |
| Example 1 | 3.38 | 0.508 | 59.5 | 24.9 | 1482 | 40% |
| Paper [17] | 2.94 | 1.0 | 40.5 | 49.2 | 1993 | - |
| Example 2 | 3.38 | 0.508 | 22.3 | 42.5 | 948 | 52% |

the sizes of the circuits in this study with those of the filters in [1] and [17]. It reveals that the sizes of the proposed filters are nearly half as small as those of the filters presented before. All the works are completed on a personal computer with a 2.4-GHz microprocessor. The computing time of the two examples is 6 and 3 min, respectively.

IV. CONCLUSIONS

An optimization scheme based on hybrid-coded GA techniques has been presented to design compact and high-performance dual-band bandpass filters. This scheme is capable of simultaneously searching appropriate circuit topology and the corresponding electrical parameters with dual-band characteristic. Two filters have been designed and implemented to validate the proposed algorithm and both filters have manifested fairly good frequency responses and compact sizes. Future work will be in introducing new simple networks such as lumped *RLC* elements, as well as active devices to the proposed representation scheme for describing general passive and active microwave circuits. The proposed algorithm will then be extended to synthesize more microwave circuits like broad-band matching networks and broad-band amplifiers.

APPENDIX A

Algorithm for Checking the Circuit Topology
Represented by a Chromosome

- Step 1) Remove all *Empty* genes in a chromosome and regenerate a new set of structures $\{\mathbf{g}_0, \mathbf{g}_1, \dots, \mathbf{g}_{M'-1}\}$.
- Step 2) Set $i = 0$.
- Step 3) If $Conn(\mathbf{g}_i) = 1$, return an error message.
- Step 4) If $Conn(\mathbf{g}_{i+1}) = 1$, go to step 5. Otherwise set $i = i + 1$ and go to Step 6).
- Step 5) If $Type(\mathbf{g}_i) \in [2, 5]$, return an error message. Otherwise set $i = i + 2$.
- Step 6) If $i \geq M' - 1$, go to next step. Otherwise go to Step 3).
- Step 7) Set $i = 0$ and $a = 0$.
- Step 8) If $Type(\mathbf{g}_i) \in [2, 6]$ or $Conn(\mathbf{g}_i) = 1$, set $a = a + 1$ and return an error message if $a > 2$.
- Step 9) If $Type(\mathbf{g}_i) = 0$ and $Conn(\mathbf{g}_i) = 0$, set $a = 0$.
- Step 10) If $Type(\mathbf{g}_i) = 1$ and $Conn(\mathbf{g}_i) = 0$, set $a = 1$. Set $i = i + 1$. If $i = M'$, terminate. Otherwise go to Step 8).

APPENDIX B

Algorithm for Evaluating Scattering
Parameters of a Chromosome

- Step 1) Remove all *Empty* genes in a chromosome and regenerate a new set of structures $\{\mathbf{g}_0, \mathbf{g}_1, \dots, \mathbf{g}_{M'-1}\}$.
- Step 2) Set $i = 0$ and $\mathbf{T} = \mathbf{I}$.
- Step 3) For $i \neq (M' - 1)$, if $Conn(\mathbf{g}_{i+1}) = 1$, go to Step 5).
- Step 4) Evaluate \mathbf{T}' where $\mathbf{T}' = ABCD(\mathbf{g}_i)$. Go to Step 6).
- Step 5) Evaluate \mathbf{Y}_i , \mathbf{Y}_{i+1} , and \mathbf{T}' where $\mathbf{Y}_i = Y(\mathbf{g}_i)$, $\mathbf{Y}_{i+1} = Y(\mathbf{g}_{i+1})$, and $\mathbf{T}' = Y2ABCD(\mathbf{Y}_i + \mathbf{Y}_{i+1})$. Set $i = i + 1$.
- Step 6) Set $\mathbf{T} = \mathbf{T} \cdot \mathbf{T}'$ and $i = i + 1$. If $i = M'$, go to Step 7). Otherwise go to Step 3).
- Step 7) Evaluate \mathbf{S} where $\mathbf{S} = ABCD2S(\mathbf{T})$.

In the above algorithms, M' denotes the number of non-*Empty* genes in a chromosome, $Type(\mathbf{g}_i)$ returns an integer representing the circuit topology of structure \mathbf{g}_i , $Conn(\mathbf{g}_i)$ returns an integer representing the connection method of structure \mathbf{g}_i , $Y(\mathbf{g}_i)$ evaluates the Y matrix of structure \mathbf{g}_i and returns the matrix, $ABCD(\mathbf{g}_i)$ evaluates the $ABCD$ matrix of structure \mathbf{g}_i and returns the matrix, $Y2ABCD(\mathbf{Y})$ converts the Y matrix \mathbf{Y} to an $ABCD$ matrix and returns the $ABCD$ Matrix, $ABCD2S(\mathbf{T})$ converts the $ABCD$ matrix \mathbf{T} to an S matrix and returns the S Matrix.

ACKNOWLEDGMENT

The circuits were fabricated and measured at the National Chiao Tung University, Hsinchu, Taiwan, R.O.C. The authors wish to express their sincere gratitude to Prof. R.-B. Hwang, and Prof. E. Y. Chang, both of the National Chiao Tung University,

for generously providing facilities for the experiments. Moreover, the authors are indebted to Prof. J.-D. Tseng, National Chin-Yi Institute of Technology, Taichung County, R.O.C., for valuable ideas about the hairpin structure. The authors further wish to express their gratitude to Prof. T.-G. Ma, National Taiwan University of Science and Technology, Taipei, Taiwan, R.O.C., for reading this paper's manuscript and making a number of valuable comments and T.-C. Pu, National Chiao Tung University, and P.-H. Deng, National Taiwan University, Taipei, Taiwan, R.O.C., for the helpful discussions.

REFERENCES

- [1] L.-C. Tsai and C.-W. Hsue, "Dual-band bandpass filters using equal-length coupled-serial-shunted lines and Z -transforms technique," *IEEE Trans. Microw. Theory Tech.*, vol. 52, no. 4, pp. 1111–1117, Apr. 2004.
- [2] K. Wada, Y. Yamamoto, and O. Hashimoto, "Design of bandpass filters with a function to control the number of the attenuation pole," *IEICE Trans. Electron.*, vol. E.85-C, no. 3, pp. 578–585, Mar. 2002.
- [3] K. Wada, K. Nakagawa, O. Hashimoto, and H. Harada, "Technique for improving out-of-band characteristics of planar microwave filters using tapped resonators," *IEICE Trans. Electron.*, vol. E85-C, no. 2, pp. 391–399, Feb. 2002.
- [4] K. Wada and O. Hashimoto, "Fundamentals of open-ended resonators and their application to microwave filters," *IEICE Trans. Electron.*, vol. E83-C, no. 11, pp. 1763–1775, Nov. 2000.
- [5] J. W. Bandler, R. M. Biernacki, S. H. Chen, D. G. Swanson, and S. Ye, "Microstrip filter design using direct EM field simulation," *IEEE Trans. Microw. Theory Tech.*, vol. 42, no. 7, pp. 1353–1359, Jul. 1994.
- [6] J. W. Bandler, A. S. Mohamed, M. H. Baka, K. Madsen, and J. Sondergaard, "EM-based optimization exploiting partial space mapping and exact sensitivities," *IEEE Trans. Microw. Theory Tech.*, vol. 50, no. 12, pp. 2741–2750, Dec. 2002.
- [7] J. W. Bandler, Q. S. Cheng, N. K. Nikolova, and M. A. Ismail, "Implicit space mapping optimization exploiting preassigned parameters," *IEEE Trans. Microw. Theory Tech.*, vol. 52, no. 1, pp. 378–385, Jan. 2004.
- [8] J. E. Rayas-Sánchez, "EM-based optimization of microwave circuits using artificial neural networks: The state-of-the-art," *IEEE Trans. Microw. Theory Tech.*, vol. 52, no. 1, pp. 420–435, Jan. 2004.
- [9] M.-H. Hsu and J.-F. Huang, "Annealing algorithm applied in optimum design of 2.4 GHz and 5.2 GHz dual-wideband microstrip line filters," *IEICE Trans. Electron.*, vol. E88-C, no. 1, pp. 47–56, Jan. 2005.
- [10] D. E. Goldberg, *Genetic Algorithms in Search Optimization and Machine Learning*. Reading, MA: Addison-Wesley, 1989.
- [11] M. Gen and R. Cheng, *Genetic Algorithms and Engineering Optimization*. New York: Wiley, 2000, ch. 3.
- [12] Y. Ruhmat-Samii and E. Michielssen, *Electromagnetic Optimization by Genetic Algorithms*. New York: Wiley, 1999.
- [13] H. Choo and H. Ling, "Design of broad-band and dual-band microstrip antennas on a high-dielectric substrate using genetic algorithm," *Proc. Inst. Elect. Eng.—Microwave Antennas Propag.*, vol. 50, pp. 137–142, Jun. 2003.
- [14] S. Chakravarty, R. Mitra, and N. R. Williams, "Application of a micro-genetic algorithm (MGA) to the design of broad-band microwave absorbers using multiple frequency selective surface screens buried in dielectrics," *IEEE Trans. Antennas Propag.*, vol. 50, no. 3, pp. 284–296, Mar. 2002.
- [15] P. L. Wener, R. Mitra, and D. H. Werner, "Extraction of SPICE-type equivalent circuits microwave components and discontinuities using the genetic algorithm optimization technique," *IEEE Trans. Adv. Packag.*, vol. 23, no. 1, pp. 55–61, Feb. 2000.
- [16] S. F. Peik and Y. L. Chow, "Genetic algorithms applied to microwave circuit optimization," in *Proc. Asia-Pacific Microwave Conf.*, 1997, pp. 857–860.
- [17] T. Nishino and T. Itoh, "Evolutionary generation of microwave line segment circuits by genetic algorithms," *IEEE Trans. Microw. Theory Tech.*, vol. 50, no. 9, pp. 2048–2055, Sep. 2002.
- [18] —, "Evolutionary generation of 3-D line-segment circuits with a broadside-coupled multiconductor transmission-line model," *IEEE Trans. Microw. Theory Tech.*, vol. 51, no. 10, pp. 2045–2054, Oct. 2003.
- [19] D. M. Pozar, *Microwave Engineering*. New York: Wiley, 1998, ch. 8.
- [20] L.-H. Hsieh and K. Chang, "Slow-wave bandpass filters using ring or stepped-impedance hairpin resonators," *IEEE Trans. Microw. Theory Tech.*, vol. 50, no. 7, pp. 1795–1800, Jul. 2002.

- [21] —, "Compact low-pass filters using microstrip stepped-impedance hairpin resonators," *IEEE Trans. Microw. Theory Tech.*, vol. 51, no. 1, pp. 193–199, Jan. 2003.
- [22] —, "Compact, low insertion-loss, sharp-rejection, and wide-band microstrip bandpass filters," *IEEE Trans. Microw. Theory Tech.*, vol. 51, no. 4, pp. 1241–1246, Apr. 2003.
- [23] A. E. Eiben, R. Hinterding, and R. Zbigniew, "Parameter control in evolutionary algorithm," *IEEE Trans. Evol. Comput.*, vol. 3, no. 2, pp. 124–141, Jul. 1999.



Ming-Iu Lai (S'04) was born in Kaohsiung, Taiwan, R.O.C., in 1976. He received the B.S.E.E. degree from National Taiwan University of Science and Technology, Taipei, Taiwan, R.O.C., in 1998, the M.S.E.E. degree from National Taiwan University, Taipei, Taiwan, R.O.C., in 2000, and is currently working toward the Ph.D. degree at National Taiwan University.

From 2001 to 2002, he was with the ZyXEL Communication Corporation, Hsinchu, Taiwan, R.O.C., where he was involved with signal integrity (SI) and electromagnetic interference (EMI) analyses. From 2002 to 2004, he was with the SynComm Communication Corporation, Hsinchu, Taiwan, R.O.C., and then joined the Applied Electromagnetic Research Laboratory, Microelectronics and Information System Research Center, National Chiao Tung University, Hsinchu, Taiwan, R.O.C., where he was involved with the designs of beam-steering antennas and high-frequency flip-chip packages. His current research interest includes two-dimensional/three-dimensional (2-D/3-D) microwave circuits design automation, grid computing techniques, and GAs for electromagnetic optimization designs, and time-domain numerical electromagnetics.



Shyh-Kang Jeng (M'86–SM'98) received the B.S.E.E. and Ph.D. degrees from National Taiwan University, Taipei, Taiwan, R.O.C., in 1979 and 1983, respectively.

In 1981, he joined the faculty of the Department of Electrical Engineering, National Taiwan University, where he is currently a Professor. From 1985 to 1993, he was with the University of Illinois at Urbana-Champaign, as a Visiting Research Associate Professor and a Visiting Research Professor. In 1999, he was with the Center for Computer Research in Music and Acoustics, Stanford University, Stanford, CA, for six months. His research interest includes numerical electromagnetics, UWB wireless systems, music signal processing, music information retrieval, intelligent agent applications, and electromagnetic scattering analysis.